# Structure of lipoprotein lipase in complex with GPIHBP1

Rishi Arora[a], Amitabh V. Nimonkar[b], Daniel Baird[a,1], Chunhua Wang[a], Chun-Hao Chiu[a], Patricia A. Horton[a], Susan Hanrahan[b], Rose Cubbon[b], Stephen Weldon[c], William R. Tschantz[c], Sascha Mueller[d], Reto Brunner[e], Philipp Lehr[d], Peter Meier[d], Johannes Ottl[e], Andrei Voznesensky[c], Pramod Pandey[a,2], Thomas M. Smith[a], Aleksandar Stojanovic[d], Alec Flyer[f], Timothy E. Benson[a], Michael J. Romanowski[a,3], and John W. Trauger[b,3]

[a]Chemical Biology and Therapeutics, Novartis Institutes for Biomedical Research, Cambridge, MA 02139; [b]Cardiovascular and Metabolic Disease Area, Novartis Institutes for Biomedical Research, Cambridge, MA 02139; [c]Biotherapeutic and Analytical Technologies, Novartis Institutes for Biomedical Research, Cambridge, MA 02139; [d]Global Discovery Chemistry, Novartis Institutes for Biomedical Research, 4002 Basel, Switzerland; [e]Chemical Biology and Therapeutics, 4002 Basel, Switzerland; and [f]Global Discovery Chemistry, Novartis Institutes for Biomedical Research, Cambridge, MA 02139

Edited by Ian A. Wilson, The Scripps Research Institute, La Jolla, CA, and approved April 16, 2019 (received for review November 27, 2018)

**Lipoprotein lipase (LPL) plays a central role in triglyceride (TG) metabolism. By catalyzing the hydrolysis of TGs present in TG-rich lipoproteins (TRLs), LPL facilitates TG utilization and regulates circulating TG and TRL concentrations. Until very recently, structural information for LPL was limited to homology models, presumably due to the propensity of LPL to unfold and aggregate. By coexpressing LPL with a soluble variant of its accessory protein glycosylphosphatidylinositol-anchored high-density lipoprotein binding protein 1 (GPIHBP1) and with its chaperone protein lipase maturation factor 1 (LMF1), we obtained a stable and homogenous LPL/GPIHBP1 complex that was suitable for structure determination. We report here X-ray crystal structures of human LPL in complex with human GPIHBP1 at 2.5–3.0 Å resolution, including a structure with a novel inhibitor bound to LPL. Binding of the inhibitor resulted in ordering of the LPL lid and lipid-binding regions and thus enabled determination of the first crystal structure of LPL that includes these important regions of the protein. It was assumed for many years that LPL was only active as a homodimer. The structures and additional biochemical data reported here are consistent with a new report that LPL, in complex with GPIHBP1, can be active as a monomeric 1:1 complex. The crystal structures illuminate the structural basis for LPL-mediated TRL lipolysis as well as LPL stabilization and transport by GPIHBP1.**

X-ray crystallography | LPL | GPIHBP1 | lipase

TGs move through the bloodstream in TRL particles: very-low-density lipoproteins (VLDLs) transport TGs produced by the liver, and chylomicrons transport TGs produced by the intestines from dietary fat. LPL is expressed by TG-utilizing (heart and skeletal muscle) and TG-storing (adipose) tissues and catalyzes the hydrolysis of TGs present in TRL particles. The resulting free fatty acids are taken up by the tissue and used as an energy source (in the heart and skeletal muscle) or for energy storage (in adipose), and the resulting TRL remnants are cleared from circulation by the liver or, in the case of some VLDL remnants, further metabolized into LDL by hepatic lipase (1). Hypertriglyceridemia (elevated plasma TGs) is very common and is associated with an increased risk of myocardial infarction and other adverse cardiovascular events (2). Human gene variants that increase LPL activity are associated with lower plasma TG levels and reduced risk of coronary artery disease (3–7). A gain-of-function variant of LPL (S474X) that moderately increases secretion of the protein without affecting its catalytic activity is associated with lower circulating TG concentrations and lower risk of coronary artery disease in humans (3). Loss-of-function mutations in the LPL inhibitor proteins ANGPTL3 and ANGPTL4 are also associated with lower TGs and lower risk of coronary artery disease in humans (3–7). These genetic association studies highlight the potential for therapeutics that increase LPL activity to lower the risk of cardiovascular events in the large population of people with hypertriglyceridemia. A thorough understanding of the structure and regulation of LPL will facilitate efforts to develop such therapeutics.

Proper catabolism of TRL particles by LPL is dependent on the accessory proteins LMF1 and GPIHBP1. Loss-of-function mutations in LMF1 and GPIHBP1 strongly impair LPL activity and cause severe hypertriglyceridemia (8–10). LMF1 is an endoplasmic reticulum-resident chaperone protein that is required for proper folding and secretion of LPL (8). After LPL is secreted by parenchymal cells of the heart, muscle, and adipose tissue, it initially binds to heparan sulfate proteoglycans (HSPG) in the subendothelial space. LPL subsequently binds to GPIHBP1, a membrane-bound protein expressed by capillary endothelial cells. GPIHBP1 transports LPL across the endothelial cell to the luminal side of the capillary endothelium where LPL binds to TRL particles in the bloodstream and catalyzes TRL-TG hydrolysis (10, 11). In the absence of functional GPIHBP1, LPL accumulates in the subendothelial space where it cannot interact with TRL particles (12).

## Significance

**LPL is the central enzyme in TG metabolism. We report here X-ray crystal structures of LPL in complex with its accessory protein GPIHBP1, including a structure with a novel inhibitor bound in the LPL active site. The inhibitor-bound structure includes the LPL lid and lipid-binding regions, which makes this the first complete crystal structure of LPL and provides insight into how these regions of LPL contribute to the recognition of TRL substrates. The structural evidence and additional biochemical experiments presented here are consistent with a newly published report that LPL, in complex with GPIHBP1, can be active as a monomeric 1:1 complex and, therefore, help overturn the long-standing assumption that LPL is only active as a homodimer.**

Author contributions: D.B., P.L., P.M., J.O., A.V., P.P., T.M.S., A.S., A.F., T.E.B., M.J.R., and J.W.T. designed research; R.A., A.V.N., D.B., C.W., C.-H.C., P.A.H., S.H., R.C., S.W., W.R.T., S.M., R.B., P.L., and A.S. performed research; R.A., A.V.N., W.R.T., P.L., and J.O. analyzed data; and R.A., A.V.N., M.J.R., and J.W.T. wrote the paper.

Conflict of interest statement: All authors are current or former employees of Novartis Institutes for Biomedical Research or Novartis Pharma AG, and some are also shareholders of Novartis. This work was funded by Novartis Institutes for Biomedical Research.

This article is a PNAS Direct Submission.



Data deposition: The atomic coordinates and structure factors have been deposited in the Protein Data Bank, www.wwpdb.org (PDB ID codes 6OAZ, 6OAU, and 6OB0).

[1]Present address: Casma Therapeutics, Cambridge, MA 02139.

[2]Present address: Experimental and Chemical Biology, Merck Exploratory Science Center, Cambridge, MA 02141.

[3]To whom correspondence may be addressed. Email: michael.romanowski@novartis.com or john.trauger@novartis.com.

This article contains supporting information online at www.pnas.org/lookup/suppl/doi:10.1073/pnas.1820171116/-/DCSupplemental.

Published online May 9, 2019.

Structural homology modeling (13–15) and a recently reported X-ray crystal structure of LPL bound to GPIHBP1 (16) indicate that LPL has a similar overall structure as pancreatic lipase (PL) and consists of a N-terminal catalytic domain (NTD) with an α/β-hydrolase fold and a C-terminal domain (CTD) with a β-sandwich fold (13–16). In contrast to PL, which is monomeric, LPL has been reported to be homodimeric with a head-to-tail orientation (15, 17–19). Furthermore, active LPL homodimers have been reported to spontaneously dissociate into inactive monomers (17, 19). In contrast, a new publication reevaluated these findings and concluded that LPL and LPL in complex with GPIHBP1 can be active as a monomer (20). GPIHBP1 has two domains—a N-terminal acidic domain in which most of the amino acids are aspartate or glutamate (21 of 26 amino acids in the human protein) and a three-fingered Ly6/uPAR (LU) domain. The LU domain is followed by a C-terminal GPI membrane anchor attachment sequence (10). Recombinant GPIHBP1 with a C-terminal truncation that eliminates the GPI attachment site [soluble GPIHBP1 (sGPIHBP1)] has been used to show that GPIHBP1 binds to LPL with high affinity, stabilizes LPL against spontaneous unfolding, and interferes with the ability of ANGPTL3 and ANGPTL4 to inhibit LPL (21–23).

In this paper, we present crystal structures of LPL in complex with sGPIHBP1. Our initial ligand-free crystal structures of the LPL/sGPIHBP1 complex are very similar to the structure recently reported by Birrane et al. (16), including the absence of most of the lid and lipid-binding regions of LPL. We subsequently determined the crystal structure of LPL/sGPIHBP1 with a novel inhibitor bound in the LPL active site. With the inhibitor bound, the lid and lipid-binding regions became ordered and visible in the structure, thus providing the first complete crystal structure of LPL and providing insight into how the lid and lipid-binding regions contribute to TRL substrate recognition. Analysis of LPL–LPL contacts in the crystal structures, enzyme activity data, and molecular mass assessment by size exclusion chromatography coupled with multiangle light scattering (SEC-MALS) were consistent with the newly published report that LPL can be active as monomer (20).

## Results

**Preparation of the LPL/sGPIHBP1 Complex.** We initially expressed human LPL using transiently transfected HEK293-F cells with heparin added to the medium and purified LPL from the conditioned medium by heparin affinity chromatography. LPL prepared in this manner was obtained with low yield (~0.3 mg per liter of culture), and SEC showed that the protein was aggregated. Although this preparation of LPL was initially enzymatically active, it completely lost activity after incubation at room temperature for 10 h (*SI Appendix*, Fig. S1). Since GPIHBP1 had been reported to stabilize LPL (22, 23), we coexpressed His-tagged human LPL and human sGPIHBP1 and, after purification by $Ni^{2+}$ affinity chromatography followed by SEC, obtained a homogenous LPL/sGPIHBP1 complex with low yield (~0.5 mg/L). Since LMF1 is necessary for proper LPL folding in vivo, we next coexpressed human LPL, sGPIHBP1, and LMF1 and after $Ni^{2+}$ affinity chromatography followed by SEC obtained a homogenous LPL/sGPIHBP1 complex with good yield (~6 mg/L). The enzyme activity of the complex was eightfold higher than that of LPL purified by heparin affinity chromatography, which could be due to the ability of GPIHBP1 to prevent unfolding of the LPL hydrolase domain (23) and aggregation and/or the different methods used to purify free LPL and the LPL/sGPIHBP1 complex. Furthermore, enzymatic activity was retained during incubation at room temperature for 10 h (*SI Appendix*, Fig. S1). To further assess stability, the LPL/sGPIHBP1 complex was immobilized on a surface plasmon resonance (SPR) chip via a biotin tag at the C-terminal end of sGPIHBP1. No dissociation of LPL from sGPIHBP1 was observed during incubation at room temperature for 8 h (*SI Appendix*, Fig. S2), indicating that the complex has a very slow dissociation rate under these conditions. When low-molecular weight heparin was added at a concentration of 5 μM, dissociation of LPL from

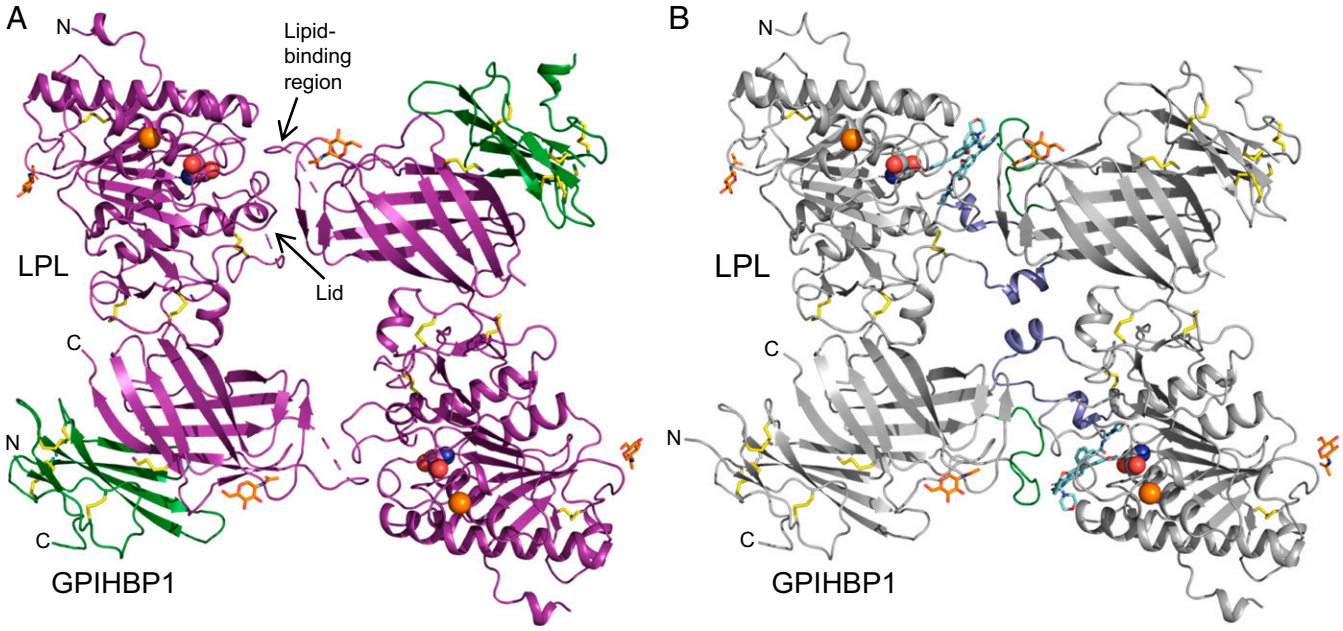


**Fig. 1.** Crystal structures of LPL/sGPIHBP1 and LPL-**2**/sGPIHBP1. (*A*) Ligand-free LPL/sGPIHBP1 structure in space group $C_12_1$ showing the head-to-tail arrangement of two LPL molecules in the asymmetric unit. The active site serine residue is represented with a space-filling model, and the bound $Ca^{2+}$ ion is represented by a sphere. The N-terminal acidic domain of GPIHBP1 and portions of the lid and lipid-binding regions of LPL (indicated by dashed lines) are not visible in the crystal structure. (*B*) Structure of the LPL-**2**/sGPIHBP1 complex in space group $P2_12_12$ in which two molecules of **2** are bound to the active site. Two of the four LPL/sGPIHBP1 complexes in the asymmetric unit are shown to illustrate the head-to-tail arrangement of LPL molecules. The LPL lid (highlighted in green) and lipid-binding region (highlighted in blue) are visible in the crystal structure. As in the ligand-free structure, the N-terminal acidic domain of GPIHBP1 is not visible.

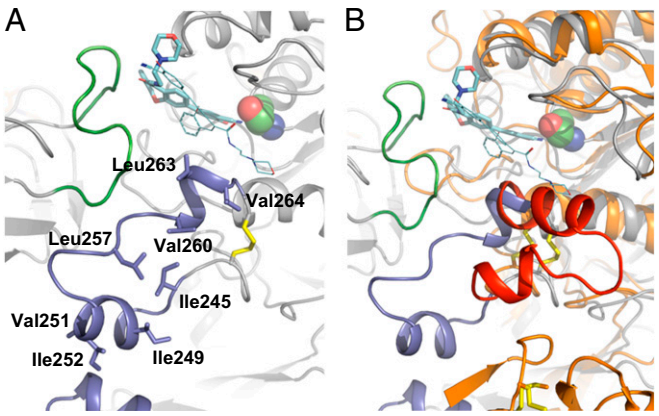


**Fig. 2.** (*A*) The lid region of LPL (highlighted in blue) in the LPL-**2**/sGPIHBP1 structure. The active site serine residue is shown as a space-filling model, and the lipid-binding region from the adjacent LPL molecule is highlighted in green. (*B*) Alignment of LPL with PL with a focus on the lid region. PL is shown in orange with its lid region highlighted in red.

sGPIHBP1 was observed (*SI Appendix*, Fig. S2), which was consistent with previous data showing that heparin and GPIHBP1 bind competitively to LPL (24).

**Crystal Structures of the LPL/sGPIHBP1 Complex.** We obtained crystals of the LPL/sGPIHBP1 complex produced in HEK293-F cells but found that these crystals only diffracted to a resolution of ∼9 Å. After expressing LPL/sGPIHBP1 in GnTI-deficient HEK293-F cells (to limit glycosylation on LPL and sGPIHBP1), we obtained crystals that diffracted to a resolution of 4.5 Å. Systematic mutation of N-linked glycosylation sites on the complex revealed that the primary glycosylation site on sGPIHBP1 (Asn78) and a secondary glycosylation site (Asn82, which is glycosylated only when Asn78 is mutated) could be mutated to aspartic acid without affecting the expression yield or enzymatic activity. In contrast, mutating either of the two N-linked glycosylation site asparagines on LPL to aspartic acid resulted in poor expression yields and aggregated protein. The complex of wild-type LPL with non-glycosylated sGPIHBP1(N78D/N82D) obtained by coexpression using HEK293-F cells or GnTI-deficient HEK293 cells (to limit glycosylation on LPL) yielded crystals that diffracted to a resolution of up to 3.0 and 2.5 Å, respectively, and provided datasets that led to a structure solution.

The initial structure of the LPL/sGPIHBP1(N78D/N82D) complex was determined at 3.0 Å resolution from protein produced in HEK293-F cells, which crystallized in the $P2_12_12$ space group (PDB ID code 6OAZ). The structure was solved using the molecular replacement method with a human PL crystal structure (PDB ID code 1lpa) (25) as the starting model for LPL and the solution structure of human CD59 (PDB ID code 2j8b) (26) as the starting model for GPIHBP1. There were four LPL/sGPIHBP1 complexes in the asymmetric unit with a head-to-tail orientation (*SI Appendix*, Fig. S3). One of the four sGPIHBP1 chains in the asymmetric unit had very poor electron density and was modeled using noncrystallographic symmetry mates. A second structure of LPL/sGPIHBP1 was determined at 2.5 Å resolution using LPL/sGPIHBP1(N78D/N82D) complex produced in GnTI-deficient HEK293 cells, which crystallized in the $C_12_1$ space group (PDB ID code 6OAU) (Fig. 1*A* and *SI Appendix*, Fig. S4). There were two LPL/sGPIHBP1 complexes in the asymmetric unit in the same head-to-tail orientation observed in the first structure; the overall packing was similar for both structures. The two structures are essentially identical, but the $C_12_1$ structure offers more details due to higher resolution. In both structures, much of the tryptophan-rich lipid-binding region of LPL (residues 412–423), much of the lid region of LPL (residues 243–266), and the entire N-terminal acidic domain of GPIHBP1 (residues 21–61) are not visible in the electron density map, indicating that these regions are conformationally flexible in the crystals. These structures are very similar to that recently reported by Birrane et al. (16) in which these regions of the protein were also missing from the electron density map.

A third structure of the complex was obtained by soaking a novel LPL inhibitor, compound **2**, into the $P2_12_12$ crystals; this structure had a resolution of 2.8 Å (PDB ID code 6OB0) (Fig. 1*B* and *SI Appendix*, Fig. S5). We initially tried to soak or cocrystallize the LPL/sGPIHBP1 complex with the known covalent inhibitors orlistat or C11 alkyl phosphonate (PDB ID code 1lpb) (27), but these efforts always resulted in ligand-free structures. By screening for compounds that bind to the LPL/sGPIHBP1 complex, we identified **2** and showed that this compound binds to the complex with low affinity ($K_D$ ∼ 11 μM) and inhibits LPL enzyme activity (*SI Appendix*, Fig. S6). In the LPL-**2**/sGPIHBP1 structure, two molecules of **2** are bound in the active site with one molecule forming H-bonding interactions with the active sites Ser159 and His268, whereas the second molecule sits above the first (*SI Appendix*, Fig. S5). Binding of **2** to LPL ordered both the lipid-binding and the lid regions such that all of the previously unresolved residues of LPL were detected; therefore this LPL-**2**/sGPIHBP1 structure is the first complete crystal structure of LPL. Binding of **2** also improved the resolution of diffraction past 3.0 Å, yielding higher atomic detail. One of the four sGPIHBP1 chains in the asymmetric unit, which previously had poor electron density, was more ordered with proper density and lower B factors compared with the other sGPIHBP1 chains.

**Architecture of the LPL-2/sGPIHBP1 Complex.** The LPL NTD has an α/β-hydrolase fold typical of lipases with one antiparallel and seven parallel β strands sandwiched between five α-helices and has four disulfide bonds and one bound $Ca^{2+}$ atom; the LPL CTD has eight antiparallel β-strands that form a β-sandwich and one disulfide bond (Fig. 1*B*). The LPL NTD (residues 28–340) includes the serine proteaselike catalytic triad (Ser159, Asp183, and His268) (*SI Appendix*, Fig. S5*B*), the oxyanion hole (Trp82 and Leu160), and the lid region (residues 245–265). The lid is in an open conformation (i.e., it is not occluding the active site) and consists of two short α-helices connected by a loop (Figs. 1*B* and 2). The LPL CTD includes the GPIHBP1 binding site (Fig. 1*B*) and the tryptophan-rich lipid-binding region (residues 412–422) that contributes to TRL substrate recognition (28) (Figs. 1*B* and 3). A surface lipophilicity representation of LPL shows that the lid and lipid-binding regions create hydrophobic patches on the surface of LPL (Fig. 4*A*). As reported by Birrane et al. (16), one of the faces of the CTD β-sandwich and the adjacent region of

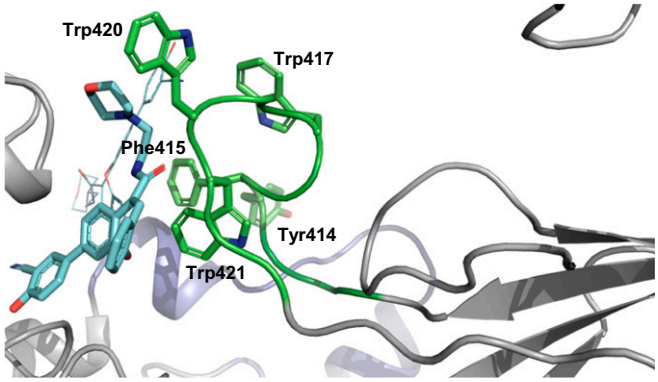


**Fig. 3.** The lipid-binding region (highlighted in green) of LPL in the LPL-**2**/sGPIHBP1 structure. The lid region of the adjacent LPL molecule is highlighted in blue.

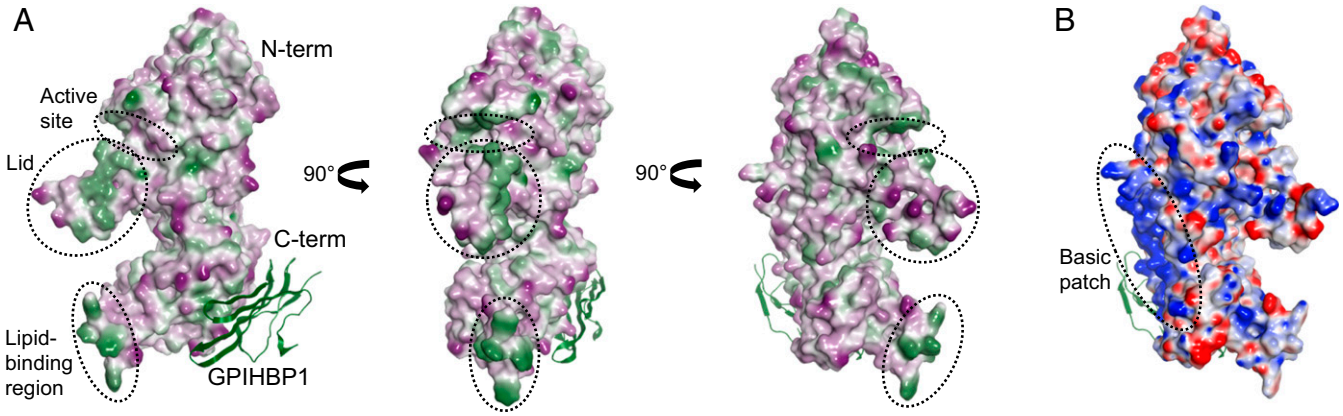


**Fig. 4.** Surface representations of LPL in the LPL-**2**/sGPIHBP1 structure (compound **2** is not shown). (*A*) LPL lipophilicity surface. Green, violet, and white shadings represent hydrophobic, hydrophilic, and neutral surfaces, respectively. (*B*) LPL electrostatic surface. Red, blue, and white shadings represent acidic (negative), basic (positive), and neutral surfaces, respectively.

the NTD has a large positively charged surface (Fig. 4*B*) that is the binding site for HSPG and the N-terminal acidic domain of GPIHBP1 (which is disordered and not visible in the structure). The LPL glycosylation sites Asn70 on the NTD and Asn386 on the CTD show complete electron density for the first GlcNAc and partial density for the second GlcNAc.

As noted above, the acidic N-terminal domain of sGPIHBP1 (residues 21–61) is disordered and not visible in the structure, which is presumably due to dynamic interaction with the large basic patch on the LPL CTD and the adjacent region of the NTD. The sGPIHBP1 three-fingered LU domain is a rather flat moiety with four antiparallel β-strands stabilized by five disulfide bonds with one face binding to the LPL CTD and the other solvent exposed (Figs. 1*B* and 4). The C-terminal LU domain of GPIHBP1 binds at an angle to LPL via a protein–protein interface that buries a hydrophobic patch on LPL. The hydrophobic core of the LPL-GPIHBP1 interface is supported by a number of hydrogen bonds and salt bridges (*SI Appendix*, Fig. S7 and Table S2).

**LPL–LPL Contacts.** Analysis of the buried surface area for LPL–LPL protein–protein contacts by PISA (29) did not reveal an obviously physiological protein–protein interface based on the relatively small buried surface areas. In the ligand-free structures, the LPL molecules adopt a head-to-tail arrangement in the asymmetric unit with the amino acids Trp420 and Trp421 from the lipid-binding region located in the active site of the neighboring molecule close to Ser159 (Fig. 5*A*). The protein–protein contacts in this region of the protein (not including the missing residues in the lid and lipid-binding regions) buried 860 Å$^2$, which correspond to 4.4% of the total accessible surface area. Apart from the Trp420-Trp421 interaction with the active site, the other notable LPL–LPL contact was a head-to-head contact involving N-terminal residues 31–69 with a buried surface area of 600 Å$^2$, which corresponds to 3.2% of the total accessible surface area. In the LPL-**2**/sGPIHBP1 structure, the lipid-binding region is folded back, out of the active site of the adjacent LPL molecule with two molecules of compound **2** bound to the active site (Fig. 5*B*). In this structure, which includes all of the lid and the lipid-binding region and in which Trp420 and Trp421 are displaced from the active site, the interfacial buried surface area for the contacts in the vicinity of the active site and lid (not including contacts with **2**) was 1130 Å$^2$, which was only 5.5% of the total accessible surface area. In sum, evaluation of buried surface areas for LPL–LPL interfaces in the ligand-free and **2**-bound crystal structures did not indicate the presence of an obviously physiological LPL–LPL protein–protein interface.

Since analysis of LPL–LPL contacts in the crystal structures did not reveal an obviously physiological protein–protein interface, we hypothesized that LPL, in complex with sGPIHBP1, may exist in solution as a monomeric 1:1 complex rather than as a homodimer 2:2 complex. To evaluate this hypothesis, we measured the molecular mass of the LPL/sGPIHBP1 complex in solution using SEC-MALS. The calculated molecular masses for the monomeric 1:1 complexes Avi-His$_6$-FLAG-LPL/sGPIHBP1 and LPL/sGPIHBP1(N78D/N82D), assuming 2.0 kDa per N-linked glycosylation site, were 75 and 69 kDa, respectively. The observed molecular masses determined by SEC-MALS were 83 kDa for Avi-His$_6$-FLAG-LPL/sGPIHBP1 and 75 kDa for LPL/sGPIHBP1 (N78D/N82D), which were consistent with a 1:1 complex (Fig. 6 and Table 1). Note that the molecular mass of LPL/sGPIHBP1 complexes could not be accurately estimated from the SEC elution time relative to standard proteins because LPL/sGPIHBP1 interacted with the SEC column (evidenced by the trailing left side of the elution peak and the broadness of the elution peak) (Fig. 6).

## Discussion

Despite the central role of LPL in the lipoprotein metabolism and despite having been first studied more than 50 y ago, until very recently (16), structural information about LPL was limited to homology models (15), presumably due to the tendency of purified LPL to unfold and aggregate. Although LPL can be stabilized by binding to heparin (22), no experimentally determined structures of LPL bound to heparin have been reported. In 2007, it was discovered that GPIHBP1 is essential for proper lipolytic processing of TRLs and that GPIHBP1 binds to LPL (30). It was also discovered that LPL activity in vivo depends on the endoplasmic reticulum-resident chaperone protein LMF1 (31).

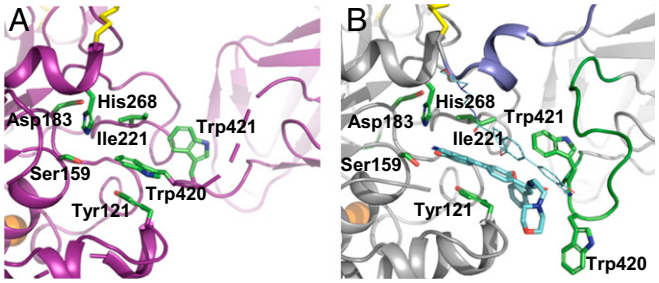


**Fig. 5.** (*A*) Detail of the head-to-tail interaction between adjacent LPL molecules in the ligand-free LPL/sGPIHBP1 structure in space group $C_12_12_1$. (*B*) In the LPL-**2**/sGPIHBP1 structure, binding of **2** to the active site displaces Trp420 and Trp421 from the active site of the neighboring LPL molecule.

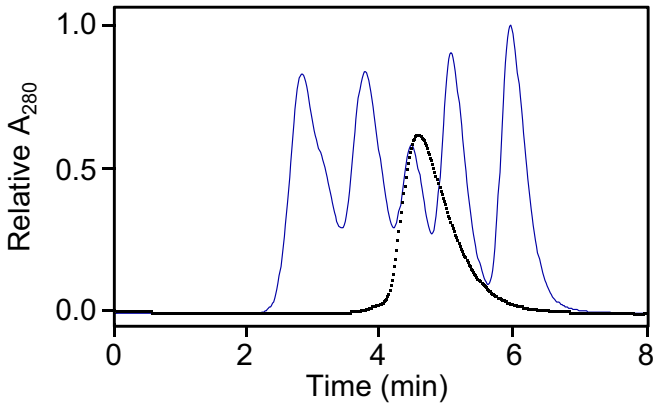


**Fig. 6.** SEC analysis of the LPL/sGPIHBP1 complex. The elution peak for Avi-$His_6$-FLAG-LPL/sGPIHBP1 (in black) is overlaid with the elution peaks for BioRad gel filtration standards (in blue). The results of MALS analysis of these elution peaks are shown in Table 1.

Subsequent work showed that GPIHBP1 could stabilize LPL from unfolding and inhibition by the endogenous inhibitor proteins ANGPTL4 and ANGPTL3 (21–23). By coexpressing LPL, LMF1, and sGPIHBP1 in HEK293-F cells, we obtained a stable, homogenous, and enzymatically active LPL/sGPIHBP1 complex. Although wild-type LPL/sGPIHBP1 crystals did not diffract to high resolution, crystals of the complex of wild-type LPL with non-glycosylated sGPIHBP1 (obtained by expression in HEK293-F cells or GnTI-deficient HEK293-F cells) diffracted well and enabled determination of X-ray crystal structures of the complex at 2.5–3.0 Å resolution, including a structure with the novel inhibitor **2** bound in the active site of LPL. In their recently reported crystal structure of the LPL/sGPIHBP1 complex (16), Birrane et al. used a different approach to prepare the complex: they prepared LPL and sGPIHBP1 separately (LPL was coexpressed with LMF1 in CHO cells, and sGPIHBP1 was expressed in *Drosophila* S2 cells) and then combined the proteins to generate the complex.

The ligand-free crystal structures of the LPL/sGPIHBP1 complex reported here (Fig. 1*A* and *SI Appendix*, Fig. S3) are very similar to the structure recently reported by Birrane et al. (16), including the head-to-tail arrangement of LPL molecules in the asymmetric unit. As in the structure of Birrane et al., in the ligand-free structures reported here electron density is missing for much of the lid and lipid-binding regions of LPL as well as the N-terminal acidic domain of GPIHBP1, indicating that these regions can adopt multiple conformations in the crystal. However, we were able to detect part of the lipid-binding region (Asp419-Ser422) and directly observe the interaction of Trp420 and Trp421 with the active site of the adjacent LPL molecule in the asymmetric unit (Fig. 5*A*), whereas Birrane et al. inferred this interaction by modeling likely conformations of the lipid-binding region.

The structure reported here with **2** bound in the active site of LPL is the first LPL crystal structure that includes electron density for all of the lid and lipid-binding regions (Figs. 1*B*, 2, and 3). The lid region of PL has been shown by X-ray crystallography to undergo a conformational change between a closed conformation in which the active site is blocked by the lid and an open conformation in which the substrates can access the active site (25). The lid region of LPL has a similar length as that in PL and presumably can also adopt closed and open conformations. In the LPL-**2**/sGPIHBP1 structure, the lid is in an open conformation and has a similar secondary structure as the open lid in a crystal structure of PL, consisting of two short α-helices connected by a loop (Fig. 2) (25). However, the lid in the LPL structure extends away from the protein whereas the lid in the PL structure is folded back against the protein (Fig. 2*B*). A mutagenesis study of the LPL lid region revealed that replacement of the 22-amino acid lid with a four-amino acid linker resulted in a mutant LPL that could efficiently hydrolyze a soluble substrate, whereas enzyme activity with an insoluble triglyceride emulsion substrate was completely abolished (32). Based on these data, it was proposed that the interaction between the lid and the lipoprotein substrates may be an important contributor to substrate recognition by LPL. Consistent with a role in lipoprotein substrate recognition, we observed that the open lid in the LPL-**2**/sGPIHBP1 structure has a number of surface-exposed hydrophobic residues (Ile245, Ile249, Val251, Ile252, Leu257, Val-260, Leu263, and Val264) (Fig. 2*A*) that create a hydrophobic patch on the surface of LPL (Fig. 4*A*). The tryptophan-rich lipid-binding region of LPL has been implicated in the recognition of TRL substrates by LPL. When Trp420 and Trp421 in the lipid-binding region were simultaneously mutated to alanine, LPL was still able to efficiently hydrolyze a water-soluble substrate but retained only 6% activity relative to wild-type LPL with an emulsified lipid substrate (28). Consistent with a role in the recognition of lipoprotein substrates, the lipid-binding region has five surface-exposed hydrophobic residues (Tyr414, Phe415, Trp417, Trp-420, and Trp421) (Fig. 3) that create a second surface hydrophobic patch (Fig. 4*A*). The hydrophobic surface patches created by the open lid and the lipid-binding region are on the same face of LPL as the active site (Fig. 4*A*), which may enable LPL to bind to TRL substrates with an orientation that facilitates delivery of TRL-TG to the active site.

For many years it was generally believed that LPL is only active as a homodimer and that the dimer subunits are arranged in a head-to-tail orientation (15, 17–19). However, a new publication revisited this assumption and used analytical ultracentrifugation to show that LPL in the absence of heparin or LPL in complex with GPIHBP1 can be active as a monomer (20). The crystal structures, enzyme activity data, and SEC-MALS data reported here are consistent with the new report. A head-to-tail orientation of LPL molecules was observed in the crystal structures reported here (Fig. 1) and in the structure recently reported by Birrane et al. (16). In addition, Birrane et al. (16) reported data from small-angle X-ray scattering (SAXS) analysis of LPL/sGPIHBP1 in solution that was consistent with a homodimeric 2:2 complex. However, several considerations suggested to us that the head-to-tail orientations seen in the crystal structures may be due to crystal packing interactions rather than a physiologically relevant protein–protein interface. First, in the unliganded crystal structures, the LPL active site is blocked by the lipid-binding region of the adjacent LPL molecule (Figs. 1*A* and 5*A*) (we observed this interaction directly, whereas Birrane et al. inferred it by modeling likely conformations of the lipid-binding region), which argues

**Table 1. Molecular mass of the LPL/sGPIHBP1 complex in solution assessed by SEC-MALS**

| Analyte | Calculated or actual mass (kDa) | Mass determined by SEC-MALS (Mw, kDa) |
|---|---|---|
| Avi-$His_6$-FLAG-LPL/sGPIHBP1 | 75* | 83 |
| LPL/sGPIHBP1(N78D/N82D) | 69* | 75 |
| Standards: | | |
| Thyroglobulin (bovine) | 670† | 724 |
| γ-Globulin (bovine) | 158† | 193 |
| Ovalbumin (chicken) | 44† | 59 |
| Myoglobin (horse) | 17† | 31 |
| Vitamin B12 | 1.3† | 1.1 |

*Calculated mass for a 1:1 complex, assuming 2.0 kDa per N-linked glycosylation site.
†Stated molecular masses for Bio-Rad gel filtration standards.

against this being an enzymatically active homodimer. Birrane et al. (16) suggested that the homodimer in their crystal structure is an inactive conformation of LPL and that flexibility of the lipid-binding region (evidenced by the poorly defined electron density) may allow the lipid-binding region to be displaced from the active site upon substrate binding. In the crystal structures reported here, we did observe that, when the inhibitor **2** binds to LPL, the lipid-binding region is displaced from the active site (Fig. 5). However, the lipid-binding region displacement mechanism proposed by Birrane et al. contrasts with the canonical mechanism for lipases according to which accessibility of substrates to the active site is regulated by movement of the lid region (25). Second, our analysis of LPL–LPL contacts in the unliganded and **2**-bound crystal structures did not reveal an obviously physiologically relevant protein–protein interface based on the relatively small buried surface areas. Third, and most convincingly, SEC-MALS analysis indicated a molecular mass for the LPL/sGPIHBP1 complex in solution that was consistent with a 1:1 complex (Fig. 6 and Table 1). It is not clear why the SAXS data reported by Birrane et al. (16) was consistent with a 2:2 complex in solution; one possibility is that the relatively high protein concentration used for the SAXS experiment resulted in the formation of a weakly associated homodimeric 2:2 complex. With respect to enzyme activity, we observed that LPL/sGPIHBP1 had robust enzyme activity after SEC purification (i.e., the enzyme activity of the complex was eightfold higher than that of free LPL purified by heparin affinity chromatography) (*SI Appendix*, Fig. S1). In addition, the enzyme activity of the complex and the complex itself were very stable (*SI Appendix*, Figs. S1 and S2). Based on these observations, we think it is reasonable to assume that, in the SEC-MALS experiment, the LPL/sGPIHBP1 that eluted from the SEC column (Fig. 6) with molecular mass determined by MALS consistent with a monomeric 1:1 complex (Table 1) was still enzymatically active. In sum, the crystal structures, enzyme activity data, and SEC-MALS data reported here are consistent with the new report that LPL, in complex with GPIHBP1, can exist as an enzymatically active 1:1 complex (20) and, therefore, help to overturn the long-standing assumption in the field that LPL is only active as a homodimer.

## Materials and Methods

Human LPL/sGPIHBP1complexes were obtained by coexpressing His-tagged LPL, sGPIHBP1, and LMF1 in HEK293 freestyle suspension cells (wild-type or GnTI deficient) and purified from the medium by $Ni^{2+}$ affinity chromatography followed by SEC. Crystals in the $P2_12_12$ and $C_12_1$ space groups were obtained in 0.15 M calcium acetate and 18% PEG3350, in 0.2 M sodium malonate, 20% (vol/vol) PEG3350, and 4% (vol/vol) 2-propanol, respectively. Diffraction data were collected at the Advanced Photon Source beamline 17ID. The $P2_12_12$ structure was obtained by molecular replacement using the NTD and CTD of human PL (PDB ID code 1lpa) and human CD59 (PDB ID code 2j8b). The $C_12_1$ and compound-bound structures were obtained by rigid body refinement using the initial structure solution. SPR was performed using a Biacore T200 instrument. SEC-MALS was conducted using a GE Superdex 200 10/300GL Increase column in line with a light scattering detector (Wyatt Treos/OptilabRex). Lipase activity was measured using the EnzChek lipase substrate. A detailed description of materials and methods can be found in the *SI Appendix*.

**ACKNOWLEDGMENTS.** The synchrotron radiation experiments were performed at the Advanced Photon Source at Argonne National Laboratory. Use of the Industrial Macromolecular Crystallography Association Collaborative Access Team (IMCA-CAT) beamline 17-ID (or 17-BM) at the Advanced Photon Source was supported by the companies of the Industrial Macromolecular Crystallography Association through a contract with Hauptman-Woodward Medical Research Institute. The Advanced Photon Source is a US Department of Energy (DOE) Office of Science User Facility operated for the DOE Office of Science by Argonne National Laboratory under Contract DE-AC02-06CH11357.

1. Olivecrona G (2016) Role of lipoprotein lipase in lipid metabolism. *Curr Opin Lipidol* 27:233–241.
2. Nordestgaard BG (2016) Triglyceride-rich lipoproteins and atherosclerotic cardiovascular disease: New insights from epidemiology, genetics, and biology. *Circ Res* 118: 547–563.
3. Liu DJ, et al.; Charge Diabetes Working Group; EPIC-InterAct Consortium; EPIC-CVD Consortium; GOLD Consortium; VA Million Veteran Program (2017) Exome-wide association study of plasma lipids in >300,000 individuals. *Nat Genet* 49:1758–1766.
4. Dewey FE, et al. (2016) Inactivating variants in ANGPTL4 and risk of coronary artery disease. *N Engl J Med* 374:1123–1133.
5. Stitziel NO, et al.; Myocardial Infarction Genetics and CARDIoGRAM Exome Consortia Investigators (2016) Coding variation in ANGPTL4, LPL, and SVEP1 and the risk of coronary disease. *N Engl J Med* 374:1134–1144.
6. Stitziel NO, et al.; PROMIS and Myocardial Infarction Genetics Consortium Investigators (2017) ANGPTL3 deficiency and protection against coronary artery disease. *J Am Coll Cardiol* 69:2054–2063.
7. Dewey FE, et al. (2017) Genetic and pharmacologic inactivation of ANGPTL3 and cardiovascular disease. *N Engl J Med* 377:211–221.
8. Doolittle MH, Ehrhardt N, Péterfy M (2010) Lipase maturation factor 1: Structure and role in lipase folding and assembly. *Curr Opin Lipidol* 21:198–203.
9. Adeyo O, et al. (2012) Glycosylphosphatidylinositol-anchored high-density lipoprotein-binding protein 1 and the intravascular processing of triglyceride-rich lipoproteins. *J Intern Med* 272:528–540.
10. Fong LG, et al. (2016) GPIHBP1 and plasma triglyceride metabolism. *Trends Endocrinol Metab* 27:455–469.
11. Goulbourne CN, et al. (2014) The GPIHBP1-LPL complex is responsible for the margination of triglyceride-rich lipoproteins in capillaries. *Cell Metab* 19:849–860.
12. Davies BS, et al. (2010) GPIHBP1 is responsible for the entry of lipoprotein lipase into capillaries. *Cell Metab* 12:42–52.
13. van Tilbeurgh H, Roussel A, Lalouel JM, Cambillau C (1994) Lipoprotein lipase. Molecular model based on the pancreatic lipase x-ray structure: Consequences for heparin binding and catalysis. *J Biol Chem* 269:4626–4633.
14. van Tilbeurgh H, Sarda L, Verger R, Cambillau C (1992) Structure of the pancreatic lipase-procolipase complex. *Nature* 359:159–162.
15. Hayne CK, et al. (2018) We FRET so you don't have to: New models of the lipoprotein lipase dimer. *Biochemistry* 57:241–254.
16. Birrane G, et al. (2019) Structure of the lipoprotein lipase-GPIHBP1 complex that mediates plasma triglyceride hydrolysis. *Proc Natl Acad Sci USA* 116:1723–1732.
17. Osborne JC, Jr, Bengtsson-Olivecrona G, Lee NS, Olivecrona T (1985) Studies on inactivation of lipoprotein lipase: Role of the dimer to monomer dissociation. *Biochemistry* 24:5606–5611.
18. Iverius PH, Ostlund-Lindqvist AM (1976) Lipoprotein lipase from bovine milk. Isolation procedure, chemical characterization, and molecular weight analysis. *J Biol Chem* 251: 7791–7795.
19. Lookene A, Zhang L, Hultin M, Olivecrona G (2004) Rapid subunit exchange in dimeric lipoprotein lipase and properties of the inactive monomer. *J Biol Chem* 279:49964–49972.
20. Beigneux AP, et al. (2019) Lipoprotein lipase is active as a monomer. *Proc Natl Acad Sci USA* 116:6319–6328.
21. Reimund M, et al. (2015) Evidence for two distinct binding sites for lipoprotein lipase on glycosylphosphatidylinositol-anchored high density lipoprotein-binding protein 1 (GPIHBP1). *J Biol Chem* 290:13919–13934.
22. Sonnenburg WK, et al. (2009) GPIHBP1 stabilizes lipoprotein lipase and prevents its inhibition by angiopoietin-like 3 and angiopoietin-like 4. *J Lipid Res* 50:2421–2429.
23. Mysling S, et al. (2016) The acidic domain of the endothelial membrane protein GPIHBP1 stabilizes lipoprotein lipase activity by preventing unfolding of its catalytic domain. *eLife* 5:e12095.
24. Kristensen KK, et al. (2018) A disordered acidic domain in GPIHBP1 harboring a sulfated tyrosine regulates lipoprotein lipase. *Proc Natl Acad Sci USA* 115:E6020–E6029.
25. van Tilbeurgh H, et al. (1993) Interfacial activation of the lipase-procolipase complex by mixed micelles revealed by X-ray crystallography. *Nature* 362:814–820.
26. Leath KJ, et al. (2007) High-resolution structures of bacterially expressed soluble human CD59. *Acta Crystallogr Sect F Struct Biol Cryst Commun* 63:648–652.
27. Egloff MP, et al. (1995) The 2.46 A resolution structure of the pancreatic lipase-colipase complex inhibited by a C11 alkyl phosphonate. *Biochemistry* 34:2751–2762.
28. Lookene A, Groot NB, Kastelein JJ, Olivecrona G, Bruin T (1997) Mutation of tryptophan residues in lipoprotein lipase. Effects on stability, immunoreactivity, and catalytic properties. *J Biol Chem* 272:766–772.
29. Krissinel E (2015) Stock-based detection of protein oligomeric states in jsPISA. *Nucleic Acids Res* 43:W314–W319.
30. Beigneux AP, et al. (2007) Glycosylphosphatidylinositol-anchored high-density lipoprotein-binding protein 1 plays a critical role in the lipolytic processing of chylomicrons. *Cell Metab* 5:279–291.
31. Péterfy M, et al. (2007) Mutations in LMF1 cause combined lipase deficiency and severe hypertriglyceridemia. *Nat Genet* 39:1483–1487.
32. Dugi KA, Dichek HL, Talley GD, Brewer HB, , Jr, Santamarina-Fojo S (1992) Human lipoprotein lipase: The loop covering the catalytic site is essential for interaction with lipid substrates. *J Biol Chem* 267:25086–25091.